Speed and force validation of an improved intravaginal dynamometer design

C.S. Czyrnyj[1,2], E. Lanteigne[1], S. Boucher[1], Y. Bader[1], A. Brennan[1], D. Lomovtsev[1], M. Vandermolen[1], and L. McLean[2,3]

[1] Department of Mechanical Engineering, University of Ottawa, Ottawa, Canada
[2]Ottawa Carleton Institute of Biomedical Engineering, University of Ottawa, Ottawa, Canada
[3]School of Rehabilitation Sciences, University of Ottawa, Ottawa, Canada

Abstract— **Intravaginal dynamometry can provide reliable and objective assessment of the active and passive properties of the female pelvic floor muscles (PFMs) and associated connective tissues. This work presents a new automated intravaginal dynamometer (IVD) designed to address the limitations of many devices described in the literature, and provides a preliminary mechanical characterization and validation of the system. The new IVD includes dual (anterior and posterior) force measurement probes, minimalistic actuators to reduce IVD size and weight, off-the-shelf components optimized for cost and performance, integrated concurrent electromyography recordings, and an easy-to-use graphic user interface (GUI). IVD load measurements were validated against an Instron® Universal Tester (0-28N) and probe opening speeds were validated using video analysis. A linear regression model was used to quantify the input/output relationship in both cases (α=0.05). While the IVD exhibited -0.828 N bias in load measurements, there was a definitive linear relationship between IVD and Instron® force measurement, with a slope of 0.950 and an excellent model fit (adjR^2=1.000). The linear relationships between the GUI set speed of arm opening and true speed measured by video analysis were also excellent (0.958<adjR^2<0.991), slopes ranged from 0.874-0.980. The bias and the standard deviation of the bias of speeds ranged from -3.987mm/s to -0.809mm/s and 2.817mm/s to 1.207mm/s, respectively, generally decreasing in magnitude with increasing diameters. While fit was still excellent, speed of opening exhibited lower validity (i.e. lower slopes) at smaller apertures, which may be due to inertia effects. The IVD design presented here demonstrates valid force and speed values during bench testing.**

Keywords— **biomechanics, dynamometer, pelvic floor, muscle strength**

I. INTRODUCTION

The complex 3D architecture of the female pelvic floor muscles (PFMs) (Fig. 1) yields forces that act in multiple planes [1]. This can make assessment of PFM biomechanical properties (e.g. strength, power, stiffness, tone) difficult to perform and quantify objectively. Because certain aspects of the PFMs act transversely across the vaginal canal, the vagina provides a means of assessing the active forces and passive forces of the female pelvic floor. Several intravaginal dynamometers (IVDs) have been designed for this purpose [2]–[5]; some are hand-held [2], [5]–[7] while others are mounted on a fixed support system [8], [9]. Intravaginal dynamometry has indeed demonstrated reliable measures of active and passive PFM properties, and it has become the gold standard for PFM evaluation in research settings [10]. IVDs may help us to understand pelvic floor disorders in women, such as urinary incontinence, pelvic organ prolapse and sexual pain disorders, and are emerging as a clinical tool to monitor the progress of therapeutic interventions [11].

Most IVD designs employ two arms which are inserted into the vagina and measure forces applied on the anterior [6], [8], posterior [7], [9], or both [5] arms during active contraction or passive stretching. The two arms may have fixed aperture [5], or be mobile with the aperture controlled manually [6], [8], [9] or automatically [2], [7].

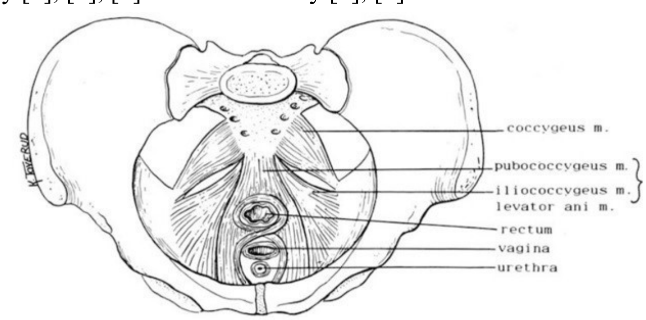

Fig. 1 The female pelvic floor muscles (PFMs) exhibit a complex 3D architecture as they span the pelvic outlet and operate with multiple lines of action [6].

While IVDs generally exhibit good reliability [2], [5]–[8], [12], there are limitations to designs in the literature. Most designs are instrumented with load cells that measure only perpendicular components of the applied force. However, the PFMs are known to act with both a “lift” and a “squeeze” action [1], suggesting that a component of the applied force is not measured with this type of instrumentation. A majority of IVD designs have only one instrumented arm. Without dual load cells providing readings on both the anterior and posterior arms, forces applied by the clinician or mounting system cannot be deducted from active and passive loads of the PFMs, yielding potential issues with validity. Devices with fixed arms are limited to the measurement of contractile force at only one muscle length, without the capacity to evaluate length-tension relationships nor passive PFM properties such as stiffness. Further, while IVDs with mobile arms can be manually controlled at low speeds, these speeds may not be adequate to study viscoelastic properties of the pelvic floor. Lastly, a majority of designs are built using customized instrumentation which is costly and limits replication of protocols.

In order to address some of these limitations, a new, lightweight, hand-held IVD built using off-the-shelf components and 3D printed casings was designed. The purpose of this work is to introduce the key features of our improved IVD and to validate its load measurement and speed control.

II. Materials and methods

A. Improved IVD Features

Key aims were to improve performance of the IVD device, decrease size and weight, and reduce manufacturing costs (Fig. 2). These aims were realized through changes to the force measurement and automated actuation systems; replacement of custom components with low-cost, off-the-shelf alternatives; addition of two concurrent electromyographic (EMG) data acquisition channels; integration of BNC outputs for live data streaming through any compatible equipment/software; and redesign of the graphical user interface (GUI).

The force measurement system was improved by the addition of a second load cell to replace an aluminum blank that previously supported the anterior arm of the IVD (EBB Series, Transducer Techniques®, Temecula, CA). This change can eliminate user-applied loads via simultaneous differential force measurements. This feature assists the user with proper positioning of the IVD during use – when the angle and position of the device are correct (i.e. at equilibrium) the forces measured by both arms are equal.

The actuator system was improved by replacing the previous single actuator with two smaller, low-weight, low-cost linear actuators (P16, Actuonix Motion Devices Inc., Victoria, BC) optimized for 0-50N loads and speeds from 14-46mm/s. The new actuators are controlled by a low cost Teensy 3.5 microcontroller (SparkFun Electronics®, Niwot, CO) with 16-bit resolution, allowing for smooth and accurate regulation of speeds and PID synchronization.

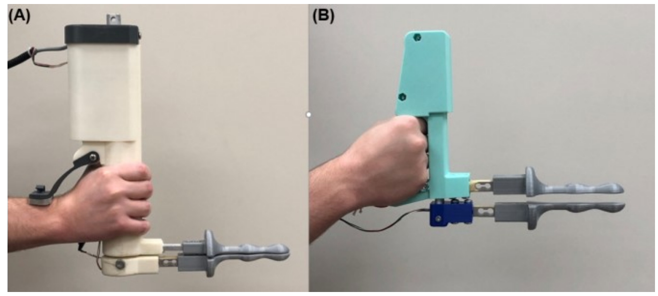

Fig. 2 (A) First generation automated intravaginal dynamometer (IVD) [14] and (B) our improved second-generation design for an automated IVD. This design is constructed using off-the-shelf components, is light (0.8kg vs.1.6kg), smaller in size, easy to operate, and is instrumented to measure force on both the anterior and posterior arms.

The analog to digital converter (Extended ADC Shield, Mayhew Labs, Indianapolis, IN), voltage regulators (S18V20AHV, Pololu Robotics and Electronics, Las Vegas, NV), and off-the-shelf amplifier chips (INA326, Texas Instruments Inc., Dallas, TX), were incorporated. Cat6 patch ISO standard ethernet crossover cables and ports, and shielded wires secured important connections and reduced noise in the system. These components are much smaller and yield a more compact, robust IVD than our previous device.

An inherent challenge of intravaginal dynamometry is differentiating forces generated by PFM contractions from those generated through bearing down maneuvers. The new IVD was modified to include two EMG channels for use with any compatible surface or intravaginal EMG electrodes. EMG data recorded from the perineum or the vagina can now be streamed simultaneously with anterior force, posterior force, and position (antero-posterior diameter) data, allowing users to confirm the presence of PFM activity during active tasks and its absence during passive elongation. This change coincided with the addition of a series of BNC outputs which allow live data streaming and storage through a range of clinical and research systems (e.g. PowerLab, ADInstruments Pty. Ltd., Sydney, AU).

The implementation of a GUI (R2018a, Matlab, The Mathworks Inc., Natick, MA) allows for data acquisition through three unique modes, active contraction, passive force and tracking tasks. In each mode, the user can specify the AP diameter to which the IVD arms open, opening velocity (10-50mm/s), hold time, and lag time before opening and after closing. Load, position and EMG data are live streamed through the GUI and data are stored as Excel files. The GUI is integrated to respond to both a software and hardware emergency stop.

B. Validation testing

Load Validation: Load validation was performed using a Universal Testing System (4482, Instron®, Norwood, MA) with a 100N static load cell (2525-807, Instron®, Norwood, MA). The IVD was held in place with arms open to 40mm (Fig. 3). An initial small impact was applied between the Instron® and the IVD in each trial, then set loads were applied to the fixed anterior arm in 2N increments increasing from 0N to 28N with three repetitions of each load. Load data from the Instron® and IVD were acquired at sampling rates of 10Hz and 28.58Hz, respectively. Data were synchronized, IVD data were resampled to 10Hz, and the last 10s of each trial were averaged to yield a single value for each device (Matlab R2016b, The Mathworks Inc., Natick, MA).

Speed Validation: Unloaded speed validation was conducted using video capture from an iPhone 6 (Apple, Cupertino, CA). The IVD was held parallel to a white wall, with a ruler in the frame, and black electrical tape was placed on the IVD arms for motion tracking. Video clips were acquired at 25-50mm apertures and at opening speeds of 10-50mm/s in 5mm and 5mm/s increments, respectively. Three repetitions were conducted at each speed. IVD arms were tracked using thresholding; the AP diameter was calculated in each frame, and time stamps were used to calculate the opening velocity from 10-90% of the set diameter (Matlab R2016b, The Mathworks Inc., Natick, MA).

Statistical Analysis: Before analysis, data were visually inspected to confirm continuity and to rule out outliers. Linear regression analyses were performed using SPSS (IBM, Armonk, NY) to evaluate the validity of IVD anterior arm load measures with respect to the Instron® data, and the speed settings with respect to video data. Histograms were used to confirm the normality assumption of the residuals and plots of predicted values against studentized residuals were used to confirm the assumptions of linearity, independence, and homoscedasticity. Bland-Altman analyses were performed to identify the distribution of errors in load and speed. Outcomes were assessed for significance (α=0.05).

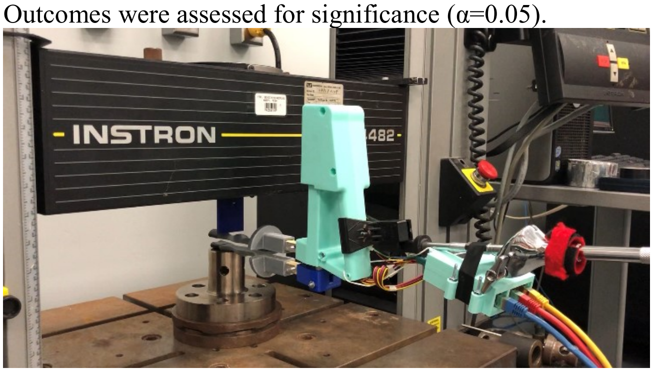

Fig. 3 Load validation on the new automated intravaginal dynamometer (IVD) was performed using the Instron® 4482.

III. Results

Load validation revealed a strong linear relationship between forces measured by the Instron® and the IVD from 0 to 28N (Fig. 5). The linear regression model suggested a perfect fit (β_0= -0.123N, β_1=0.950N/N, R^2=1.0; Table 1). Speed validation also revealed a strong linear relationship between the GUI set speed and the true speed measured by video analysis (adjR^2>0.950, Table 1).

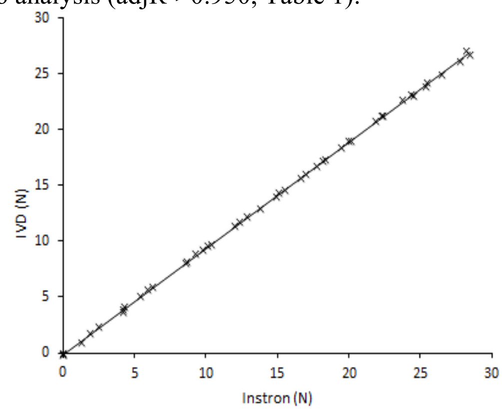

Fig. 4 Results for the load validation performed on the fixed anterior arm of the intravaginal dynamometer (IVD) against an Instron® 4482.

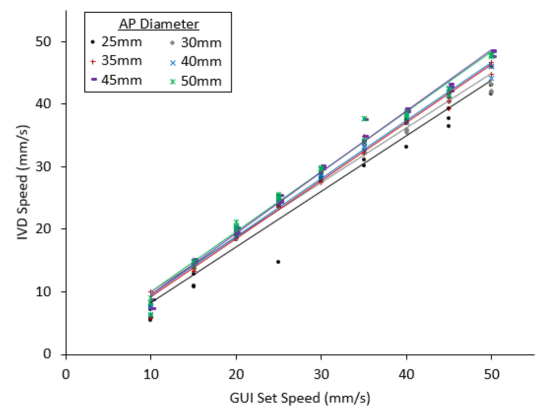

Fig. 5 GUI set speed of the intravaginal dynamometer (IVD) vs. true speed measured at different antero-posterior (AP) opening diameters.

Table 1 Validation of the new intravaginal dynamometer.

	Diameter (mm)	Slope		Intercept		Model Fit	
		β_1	p	B_0	p	AdjR^2	SEE
Load (N)	40	0.950	<0.01	-0.123	0.001	1.000	0.123
Speed (mm/s)	25	0.889	<0.01	-0.658	0.585	0.958	2.445
	30	0.874	<0.01	1.191	0.143	0.981	1.618
	35	0.930	<0.01	-0.145	0.838	0.986	1.449
	40	0.931	<0.01	0.176	0.776	0.990	1.254
	45	0.980	<0.01	-0.246	0.679	0.991	1.207
	50	0.961	<0.01	0.356	0.645	0.985	1.566

The standard error of the estimate (SEE) was low (SEE<2.5mm/s) at all speed-diameter combinations. The smallest two diameters (25mm, 30mm) yielded the lowest slopes ($ß_1$=0.889, 0.874), highest SEEs (2.445mm/s, 1.618mm/s), and poorest fit (adjR^2=0.958, 0.981). The largest two diameters (45mm, 50mm) exhibited the highest slopes ($ß_1$=0.980, 0.961), lowest SEEs (SEE=1.207 mm/s, 1.566 mm/s) and the best fit (adjR^2=0.991, 0.985). Two outliers were present in the data set, one at the 25mm aperture at the 15mm/s and 25mm/s GUI set opening speeds.

Bland-Altman analyses revealed the presence of significant biases across all diameters and loads (Table 2). While the bias for load measurement was less than 1N, bias for speed (mean difference) ranged from -4mm/s to -0.8mm/s, decreasing in magnitude with increasing diameter. The standard deviations of the biases (STDs) were less than 0.5N for the load measures, while STDs for the speed measures ranged from 2.8mm/s to 1.6mm/s, generally decreasing in magnitude with increasing diameter.

Table 1 Bland-Altman analysis results for validation of load and speed

	Diameter (mm)	Mean Difference (MD)		Error		Limits of Agreement	
		MD	p	STD	SE	LB	UB
Load (N)	40	-0.828	<0.001	0.451	0.116	-1.711	0.055
Speed (mm/s)	25	-3.987	<0.001	2.807	0.936	-9.489	1.515
	30	-2.596	<0.001	2.297	0.765	-7.098	1.906
	35	-2.247	<0.001	1.694	0.565	-5.566	1.072
	40	-1.905	<0.001	1.532	0.511	-4.907	1.097
	45	-0.852	0.001	1.207	0.402	-3.219	1.514
	50	-0.809	0.002	1.619	0.540	-3.981	2.363

IV. Discussion

We have developed a new IVD for the measurement of active force and passive PFM tissue properties. Our IVD improves upon many of the limitations of designs presented in the literature and includes improved functionality for clinical and research applications. Our results demonstrate that forces measured by the IVD are valid, and that the IVD operates within 2-4mm/s of the speed set through the GUI across a range of values. These results support the use of this IVD across a range of applied loads, diameters, and opening speeds relevant to the assessment of PFM biomechanical function.

For the load validation, the significant bias of -0.828N suggests an error in zeroing or a resistance mismatch. During our second stage of validation we will confirm that the system is accurately and reliably calibrated and zeroed. Repeated trials of the calibration and zeroing will allow us to determine the nature of and eliminate any true bias or calibration error in the system.

For the speed validation, the significant bias (range -4mm/s to -0.8mm/s), and the STD of the bias (range 2.8mm/s to 1.6mm/s) across all apertures were not surprising. With the use of low-cost, dual actuators, intended to reduce the weight and size of the IVD, we balanced the hardware limitations of the actuators by implementing a higher integral factor in our control system to allow for more tolerance. Results exhibited here are a natural consequence of this design. Our second stage of speed validation will include a higher resolution on the range of testing speeds, with a larger number of repeated trials to determine the true speed bias and STD at each diameter. Using these data, we aim to refine the integral factor in the control system and incorporate a bias correction if necessary.

The slopes, biases, and STD of biases which generally exhibited an inverse relationship to diameter were to be expected. Although the linear actuators open at a constant velocity, there is initial acceleration as opening begins and deceleration as the arms approach their set diameter. At smaller target diameters, acceleration may have occurred across the 10-90% of the set opening distance over which speed was measured. In cases of use where a smaller diameter may be indicated (e.g. pelvic pain disorders), inertia effects must be considered, particularly in the evaluation of passive tissue stiffness.

While the system performed well in this validation testing, a second stage of testing is planned. A key feature of the new IVD design is the incorporation of dual arm instrumentation to allow for optimization of IVD positioning through visual feedback. The upcoming validation tests will confirm that the live feedback from the dual-instrumented arms does indeed improve validity and reliability. Continued testing will include a loaded speed validation to ensure the control system and linear actuators operate as expected under functional loads. Further, we will confirm that the location of force application along the length of the arms does not impact the magnitude of measured loads. Lastly, accelerations of the linear actuators will be tested to better understand the constant velocity range over which validation testing should be performed, and over which passive tissue stiffness should be evaluated.

V. Conclusion

The second generation IVD showed improved functionality over its predecessor while incorporating new design features to increase functionality and performance. Our results suggest that load measurement and speed control systems are valid.

Acknowledgements

Funding for this work was provided through a Discovery Grant to Dr. McLean (RGPIN 05256-2016) from the Natural Sciences and Engineering Research Council of Canada.

Conflict of Interest

The authors declare that they have no conflict of interest.

References

[1] K. Bø *Int. Urogynecol. J. Pelvic Floor Dysfunct.*, vol. 15, no. 2, pp. 76–84, 2004.
[2] J. A. Kruger et al. *Neurourol. Urodyn.*, vol. 34, no. 2, pp. 133–138, Feb. 2015.
[3] M. Verelst and G. Leivseth *Neurourol. Urodyn.*, vol. 26, no. 6, pp. 852–857, Oct. 2007.
[4] M. Morin et al. *J. Electromyogr. Kinesiol.*, vol. 20, no. 5, pp. 795–803, 2010.
[5] J. M. Miller et al. *Neurourol. Urodyn.*, vol. 26, no. 6, pp. 858–863, Oct. 2007.
[6] M. Verelst and G. Leivseth *Neurourol. Urodyn.*, vol. 23, no. 7, pp. 662–667, 2004.
[7] M.-È. Bérubé et al. *Neurourol. Urodyn.*, pp. 1–14, Apr. 2018.
[8] F. R. Nunes et al. *Pm&r*, vol. 3, no. 1, pp. 21–26, 2011.
[9] C. Dumoulin et al. *Neurourol. Urodyn.*, vol. 22, no. 7, pp. 648–653, 2003.
[10] T. Stark et al. *PMRJ*, vol. 3, no. 5, pp. 472–479, 2011.
[11] B. Navarro Brazález et al. *Neurourol. Urodyn.*, 2017.
[12] M. Morin et al. *Neurourol. Urodyn.*, vol. 26, no. 3, pp. 397–403, 2007.